Chinese Chemical Letters 31 (2020) 1768–1772

Contents lists available at ScienceDirect

Chinese Chemical Letters

journal homepage: www.elsevier.com/locate/cclet

Review

The application of metal-organic frameworks in electrocatalytic nitrogen reduction

Yihang Wang, Qiang Li, Wei Shi*, Peng Cheng

Key Laboratory of Advanced Energy Materials Chemistry (MOE) and Collaborative Innovation Center of Chemical Science and Engineering (Tianjin), College of Chemistry, Nankai University, Tianjin 300071, China

ARTICLE INFO

Article history:
Received 11 November 2019
Received in revised form 29 December 2019
Accepted 6 January 2020
Available online 7 January 2020

Keywords:
Nitrogen reduction reaction
Metal-organic frameworks
Electrocatalysis
Nanomaterials

ABSTRACT

In recent years, the research of nitrogen reduction reaction (NRR) under ambient conditions has attracted wide attention for their relatively low energy consumption, in which rational design of electrocatalysts is the key to achieve high-performance NRR. Metal-organic frameworks (MOFs), as a new kind of porous material, have been intensively studied in the past few decades owing to not only their structural versatility and tunability but also intrinsic porosity. Due to their structural features, MOFs also have potential applications in mild condition electrocatalysis of NRR. In this review, the recently experimental and theoretical studies of MOFs in NRR electrocatalysts are briefly summarized.

1. Introduction

Ammonia is an essential raw material for modern industry, which has been industrially produced *via* the Haber-Bosch process since 1913 [1]. However, the high pressure and high temperature needed in the Haber-Bosch method make it greatly energy-consuming, contributing to 1.6%–3% of total CO_2 production of the world [2]. To achieve a more sustainable and environmentally friendly way of NH_3 production, it is important to develop new catalysts for nitrogen reduction reaction (NRR) under mild conditions [3].

The key of highly efficient NRR lies in the well understanding of the structural-property correlation of NRR catalysts [4]. In nature, N_2 is reduced to NH_3 *via* complicated processes catalyzed by a series of enzymes containing different active metal centers [5]. Inspired by the high-efficiency of nitrogenases, early research works were conducted to realize artificial N_2 fixation catalysts by mimicking their natural counterparts. However, the well-defined micro-environments and the synergistic effects between different active centers make it a great challenge to be realized in artificial systems, which also often have stability issues [6]. In contrast, heterogeneous catalysts such as doped-graphene [7], metal nanoparticles (NPs) [8], single atom catalysts (SACs) [9], single cluster catalysts (SCCs) [10] have become the new interests. However, these catalysts are faced with a common problem derived from the competition with hydrogen evolution reaction (HER). So far, the selectivity and efficiency of NRR catalysts are difficult to achieve simultaneously.

Metal-organic frameworks (MOFs), which is a hot spot in inorganic chemistry and materials science, have attracted great interest recently [11]. Compared to other catalysts, MOFs have large potential to be applied as NRR catalysts but have been rarely investigated. The suitable chemical environments of the pores or channels of MOFs could be beneficial to concentrate and activate N_2 to improve the catalytic efficiency, while the periodically arranged metal sites may serve as catalytic centers. Moreover, MOFs can be converted to or combined with other functional materials like NPs, to further enhance the catalytic performance [12]. Up to now, investigations have shown that MOFs can be applied into HER, oxygen reduction reaction (ORR) and carbon dioxide reduction reaction (CO_2RR) [13], whereas the applications of MOFs in electrocatalytic NRR are in the early stage. In this review, the existing examples of MOFs in the application of NRR were summarized as three main strategies: i) MOFs as precursors of NRR catalysts, ii) MOFs as NRR catalysts and iii) MOF-based composites as NRR catalysts.

2. MOFs as precursors of NRR catalysts

2.1. MOF-derived N-doped porous carbon (NPC)

N-Doped porous carbons (NPCs) have been extensively used as catalysts, especially in the field of electrochemical reduction. MOF-derived NPCs with high N content show good N_2 adsorption,

* Corresponding author.
E-mail address: shiwei@nankai.edu.cn (W. Shi).

https://doi.org/10.1016/j.cclet.2020.01.010
1001-8417/

tunable functionalization and tailorable morphologies, but the synthesis of NPCs is complicated and costly using traditional synthetic routes. Examples of MOF-derived NPCs have been applied to electrocatalysis, such as HER and CO_2RR [14]. In addition, by rational design and fabrication, MOF-derived NPCs can avoid the doping of transition metals which usually have HER catalytic activity, thus enhancing the selectivity for NRR.

In 2018, Quan and coworkers reported a NPC NRR catalyst synthesized *via* pyrolysis of ZIF-8 at different temperatures, as shown in Fig. 1 [15]. Scanning electron microscope (SEM) and transmission electron microscope (TEM) characterizations revealed that there was no remarkable morphological change in the carbonization process under 750–950 °C. X-ray photoelectron spectroscopy (XPS) showed that the NPC formed at 750 °C (NPC-750) has the highest N content (13.6%) and the best electrocatalytic performance, with an NH_3 production rate up to 1.40 mmol g^{-1} h^{-1} and Faradaic efficiency (FE) of 1.42% at −0.9 V *vs.* reversible hydrogen electrode (RHE). DFT calculations showed that the pyridinic and pyrrolic N-doping in NPC can introduce active sites to facilitate the N_2 bond cleavage, which is one of the main factors of the high catalytic performance.

Wu *et al.* reported another ZIF-8-derived NPC as NRR electrocatalyst with the NH_3 production rate of 4.25 mmol g^{-1} h^{-1} and FE of 10.2% at −0.3 V *vs.* RHE [16]. The reaction temperature of 1100 °C is higher than the boiling point of zinc and as a result more N_4 moieties were formed due to the evaporation of Zn. The mechanism of N_2 reduction was further elucidated with DFT calculations. The only active site for NRR was derived from the pyridinic N_3 moiety in the graphitic layer. In this mechanism, a N_2 molecule has its two nitrogen atoms protonated subsequently, during which a stable N_4 intermediate is passed through (Fig. 2). When decreasing electrode potential to −0.3 V, the activation energy is lowered, thus making the catalytic reaction more efficient.

In 2019, Song and co-workers reported an N, P co-doping carbon (NP-C-MOF-5) catalyst for NRR [17]. Through the pyrolysis of MOF-5 with dicyandiamide (DCDA) and triphenylphosphine (TPP), NP-C-MOF-5 was prepared. In NRR, NH_3 and $N_2H_4{\cdot}H_2O$ were both observed at −0.1 V *vs.* RHE with the yield rates of 0.0635 and 3.40×10^{-5} mmol g^{-1} h^{-1}. The catalytic pathway was studied by *in situ* Fourier transform infrared spectroscopy (FTIR) characterization, indicating that NP-C-MOF-5 favors the associative mechanism (Fig. 3).

2.2. MOF-derived Nanoparticle (NP)

Except for NPCs, MOF-derived NPs have also been applied as NRR catalysts which have controllable morphologies and microenvironments surrounding the active sites.

In 2018, Xu and Zou *et al.* reported a cobalt phosphide hollow nanocage (CoP HNC) derived from ZIF-67 as NRR electrocatalyst [18]. In synthesis, ZIF-67 nanocrystal was firstly solvothermally treated in the presence of Co^{2+} to form cobalt layered double hydroxide hollow nanocage, which was further converted to CoP HNC *via* thermal-assisted phosphorization with NaH_2PO_2. High FE of 7.36% at 0 V *vs.* RHE and high NH_3 production of 0.63 mmol g^{-1} h^{-1} were achieved,

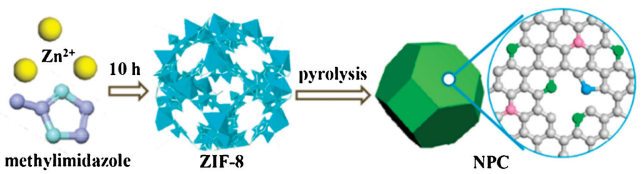

Fig. 1. Schematic illustration of NPC preparation. Copied with permission [15]. Copyright 2019, American Chemical Society.

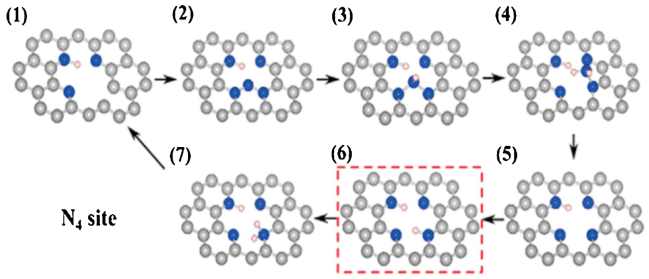

Fig. 2. Atomistic structure scheme showing the reaction pathway of the N_2 reduction on the N_3 sites. The blue, gray, and white balls represent N, C and H atoms, respectively. Copied with permission [16]. Copyright 2019, Elsevier B.V.

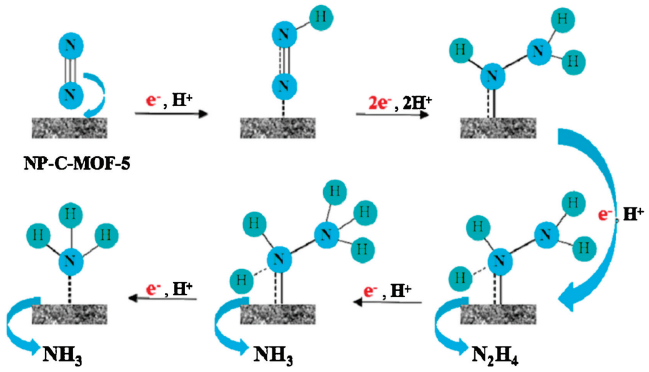

Fig. 3. Proposed reaction pathway of NRR on the NP-C-MOF-5 surface. Copied with permission [17]. Copyright 2019, American Chemical Society.

with no hydrazine byproduct. However, the competitive HER problem was not perfectly solved.

In 2019, He and co-workers reported another NRR catalyst Co@N-doped carbon (Co@NC) obtained *via* pyrolysis of ZIF-67 [19]. NH_3 production rate of 5.65×10^{-4} mmol cm^{-2} h^{-1} and FE of 21.79% were achieved. According to their results, apart from the N_3 active sites reported before [16], the Co-N_x structures in Co@NC can also participate in the activation of N_2 molecules, since the N atom in Co-N_x is similar to pyridinic N. The high surface area and abundance of active sites of Co@NC jointly realized its high catalytic efficiency. Additionally, NRR catalysts derived from MIL-88 [20], as well as other MOFs [21–24], were also prepared *via* similar hydrolysis process.

2.3. MOF-derived single-atom catalyst

Recently, single-atom catalysts (SACs) have been given great attention for diverse catalytic reactions including NRR, in which MOFs have been used as powerful precursors for SACs due to their well-defined structure and accurate designability [25].

In 2018, Zeng and co-workers reported a MOF-derived Ru single-atom catalyst for NRR [26]. By partial substitution of $Zn(NO_3)_2$ with $Ru(acac)_3$, a Ru-containing ZIF-8 precursor was synthesized and further pyrolyzed under N_2 flow to obtain Ru single atoms distributed on nitrogen-doped carbon (Ru SAs/N-C). Ru SAs/N-C shows a FE of 29.6% and a record-high NH_3 yield rate of 7.1 mmol g^{-1} h^{-1} at −0.2 V *vs.* RHE. A 12 h potentiostatic test was applied to evaluate the durability and the NH_3 yield rate decayed less than 7%. According to N_2 temperature-programmed desorption (N_2-TPD) test, the stronger binding strength between N_2 and Ru SAs/N-C is responsible for the superior catalytic performance.

In 2019, Sun *et al.* constructed a Ru@ZrO_2/NC single-atom catalyst simply by annealing Ru confined UIO-66, which showed an

NH_3 yield rate of 0.21 mmol g^{-1} h^{-1} at −0.21 V *vs.* RHE and a FE of 21% at a low overpotential of 0.17 V [27]. The current density curves remained stable over 60 h at a constant potential of −0.21 V, indicating the outstanding durability of the Ru@ZrO_2/NC. Density functional theory (DFT) calculations demonstrated that a reduced free energy for *NNH formation was beneficial for NRR process.

3. MOFs as NRR catalysts

Using MOFs directly as electrocatalysts has been given great attention recently because of the rapid development of MOF chemistry.

In 2017, Yin and co-workers reported the first application of MOFs as electrocatalysts for N_2 fixation at mild condition [28]. A series of Fe-, Co- and Cu-based MOFs were synthesized, among which the Fe-MOF displayed the best performance of NH_3 formation rate up to 7.63×10^{-3} mmol cm^{-2} h^{-1} and FE of 1.43% under 2.4 V *vs.* RHE at 90 °C. When increasing applied voltages from 1.0 V to 1.2 V, more H^+ generated and transferred to cathode to expedite the NH_3 formation, while over 1.2 V the over-saturated proton led to enhanced HER. According to their results, the MOFs with empty d-orbitals served as N_2 adsorbent and Lewis acid, which can facilitate both the enrichment and activation of N_2 molecules on the electrode surface.

In 2019, Wei and Kuang *et al*. reported another MOF catalyst for NRR [29]. MOF JUC-1000/CC acted as a versatile electrode material for both NRR on cathode and sodium gluconate (SG) oxidation on anode, as shown in Fig. 4. At 0.4 V *vs.* RHE, an NH_3 yield rate of 1.45 mmol g^{-1} h^{-1}, an FE of 11.90%, and a selectivity of 96.96% were achieved (Fig. 5). Experiments showed that the combination of SG electro-oxidation greatly enhanced the NH_3 production rate without the sacrifice of FE, mainly because of higher oxidability of SG. This proof of concept study revealed an important strategy of NRR, which guarantees high production rate and high FE simultaneously.

MOFs with planar and π-conjugated structures received particular attention for NRR, owing to their high stability, good electrical conductivity, and empty metal orbits. In 2019, Sun and co-workers reported the NRR catalytic performance of a series of conductive 2D MOFs, $TM_3(HAB)_2$ (TM = Co, Ni, Cu and Mo; HAB = hexaaminobenzene), by spin-polarized DFT calculations (Fig. 6) [30]. Among them, $Mo_3(HAB)_2$ showed the best NRR catalytic performance. The NRR *via* the distal mechanism was the most favorable one at overpotential of only 0.18 V. The first step, *i.e.*, the first hydrogenation was proved to be the rate-limiting step, with an activation energy of 0.34 eV. In addition, the weak adsorption of H_2O on $Mo_3(HAB)_2$ made it highly selective. In fact, $TM_3(HAB)_2$ with Co, Ni and Cu as metal nodes have already been

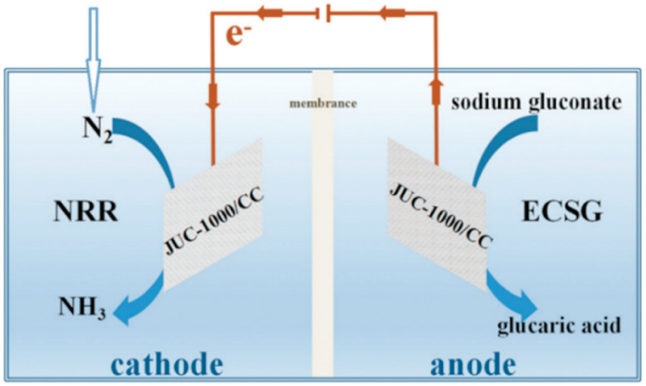

Fig. 4. Illustration of the JUC-1000/CC electrodes. Copied with permission [29]. Copyright 2019, The Royal Society of Chemistry.

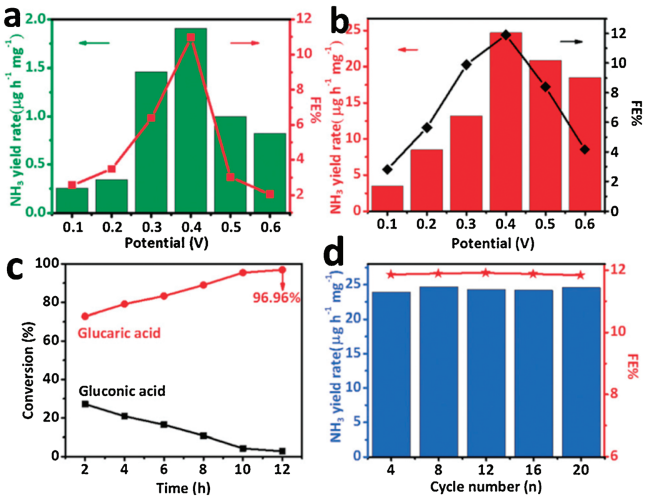

Fig. 5. Comparison of NH_3 production rates of JUC-1000/CC. (a, b) NH_3 yield rates and FEs at different potentials without SG and with SG. (c) Conversion (%) of SG and selectivity (%) of Glucaric acid (GA) at a cell voltage of 0.4 V in 1.0 mol/L Na_2SO_4 with SG. (d) Stability test results for JUC-1000/CC at 0.4 V in 1.0 mol/L Na_2SO_4 with 1.0 mol/L SG under JUC-1000/CC||JUC-1000/CC electrolytic cell device. Copied with permission [29]. Copyright 2019, The Royal Society of Chemistry.

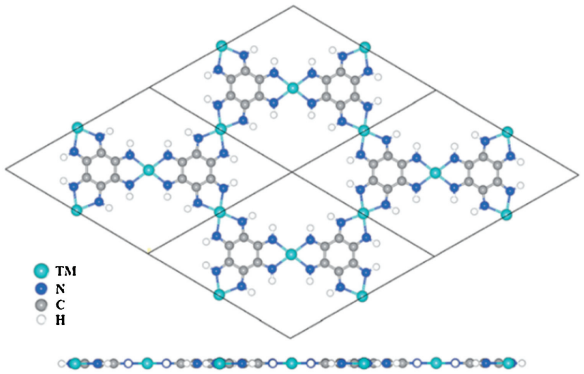

Fig. 6. Top and side views of the $TM_3(HAB)_2$. Copied with permission [30]. Copyright 2019, The Royal Society of Chemistry.

synthesized through bottom-up liquid-liquid and air-liquid interfacial reactions and a rational modified method should be able to construct $Mo_3(HAB)_2$ [31]. With the same calculation method, Liu and his co-workers studied MC_4S_4 (M = Fe, Co, Ni, Cu, Ru, Rh, Pd, Ag, Os and Ir), another promising π-conjugated 2D MOF as NRR catalyst, in which OsC_4S_4 showed an overpotential of 0.31 V (Fig. 7). According to their result, the mechanism of OsC_4S_4 catalyst was similar to $Mo_3(HAB)_2$, with an activation energy of 0.49 eV [32]. Moreover, the stability evaluation of OsC_4S_4 was carried out by molecular dynamics (MD) simulations, indicating an extremely high thermostability of 500 K. In experiments, NiC_4S_4 and CoC_4S_4 have been synthesized with an air-liquid interfacial method, however, these kinds of 2D MOFs have not been reported in experimental NRR systems, which still remains to be further investigated [33,34].

4. MOF-based composites as NRR catalysts

To overcome the shortcomings of singular NRR catalysts, the combination of metal nanoparticles and MOFs is a promising way for highly catalytic performance because of their synergistic effects. As it is difficult to achieve high NH_3 production rate while maintaining high FE, strategies have been developed using composite catalysts to

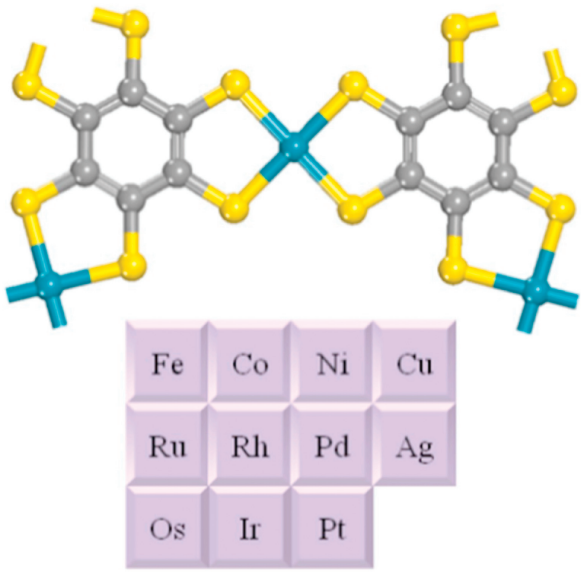

Fig. 7. Coordination structures of MC_4S_4 nanosheet, where M includes Fe, Co, Ni, Cu, Ru, Rh, Pd, Ag, Os and Ir. Copied with permission [32]. Copyright 2019, Elsevier B.V.

achieve high production rate while avoiding competitive reactions. When combining hydrophobic materials with noble metal, H_2O molecules are less likely to reach the surface of catalyst, thus reducing side reaction of HER.

In 2019, Lee and co-workers reported a reticular chemistry approach to realize both efficient and selective NRR at ambient condition [35] In their work, noble metal NPs, as highly active catalysts, were coated with a superhydrophobic ZIF-8 layer to form Ag-Au@ZIF, which was able to concentrate N_2 while repelling the water from the surface of catalysts (Fig. 8). Through this method, competitive HER was remarkably suppressed. The selectivity is up to 90%, while a large increase (10%) in FE was also achieved compared by using the metal catalyst only.

In 2019, Li and Du *et al.* also reported a nanoporous gold embedded ZIF composite (NPG@ZIF-8) for electrochemical NRR [36]. With the similar hydrophobic protection strategy, the highest FE of 44% in water electrolyte systems was achieved at −0.6 V *vs.* RHE, where the selectivity was 98%. A high NH_3 production rate of 28.7 μg cm^{-2} h^{-1} was obtained at −0.8 V *vs.* RHE.

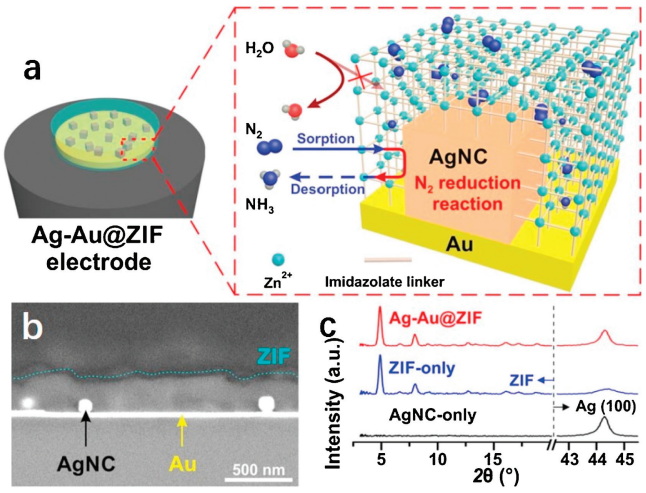

Fig. 8. Characterization of Ag-Au@ZIF. (a) Scheme of Ag-Au@ZIF as water repellent and N_2 molecular concentrator for electrochemical NRR into ammonia (inset). HCl-treated Ag nanocube is denoted as AgNC. (b) Cross-sectional SEM image of Ag-Au@ZIF with an 18-nm Au film as proxy. (c) Substrate XRD pattern of AgNC, neat ZIF thin film and as-synthesized Ag-Au@ZIF (bottom to top). Copied with permission [35]. Copyright 2019, American Association for the Advancement of Science.

5. Conclusion

In this review, three main strategies of using MOF-based or MOF-derived nanomaterials as NRR catalysts were briefly summarized. The MOF-derived catalysts have several successful examples, and their experimental methods and mechanism studies are relatively clear. MOF-derived NPCs and NPs for NRR have superiority for their controllable composition and morphology. SACs, because of their excellent activity and maximum utilization of active metal sites, should be paid more attention in the future, but it is still challenging to realize accurate control over the number of SACs and the coordination environment of the active site. For the strategy of using MOFs directly as NRR catalysts, only proof-of-concept works were reported because of the relatively low catalytic activity and stability of most of the MOFs. However, 2D MOFs with planar structure should be paid more attentions in the future because of their relatively high conductivity. For the strategy of MOF-based composites, high NRR performances can be achieved due to the synergistic effect between MOFs and other components in the catalytic composites.

The electrochemistry of NRR under ambient condition is of great interest for its energy-efficiency and environmental friendliness. The application of MOFs for NRR will become a hot spot in this burgeoning field. Up to now, the existing work only reveals a small part of the potential application of MOF-related materials in NRR and their performance is not yet comparable with noble metal catalysts at the present stage. Further investigations from both the experimental and theoretical studies are needed to obtain a high-performance catalytic performance based on a well understanding of the mechanism and improvement on both composition and morphology by the light of other known NRR catalysts.

Declaration of competing interest

The authors declare that they have no known competing financial interests or personal relationships that could have appeared to influence the work reported in this paper.

Acknowledgments

This work was supported by the National Natural Science Foundation of China (No. 21421001), the Natural Science Foundation of Tianjin (No. 18JCJQJC47200) and the Fundamental Research Funds for the Central Universities.

References

[1] P.Morrison Philip, Am. Sci. 87 (1999) 542–553.
[2] M. Kitano, Y. Inoue, Y. Yamazaki, et al., Nat. Chem. 4 (2012) 934–940.
[3] B.H.R. Suryanto, H. Du, D. Wang, et al., Nat. Catal. 2 (2019) 290–296.
[4] H. Liu, L. Wei, F. Liu, et al., ACS Catal. 9 (2019) 5245–5267.
[5] S.L. Foster, S.I.P. Bakovic, R.D. Duda, et al., Nat. Catal. 1 (2018) 490–500.
[6] X. Yan, D. Liu, H. Cao, et al., Small Methods 3 (2019) 1800501.
[7] X. Liu, L. Dai, Nat. Rev. Mater. 1 (2016) 16064.
[8] H. Mistry, A. Varela, S. Kühl, P. Strasser, B. Cuenya, Nat. Rev. Mater. 1 (2016) 16009.
[9] X. Yang, A. Wang, B. Qiao, et al., Acc. Chem. Res. 46 (2013) 1740–1748.
[10] L. Liu, A. Corma, Chem. Rev. 118 (2018) 4981–5079.
[11] H. Furukawa, K. Cordova, M.O.' Keeffe, O. Yaghi, Science 341 (2013) 974–975.
[12] Y. Xue, S. Zheng, H. Xue, H. Pang, J. Mater. Chem. A 7 (2019) 7301–7327.
[13] J. Liu, S. Hou, W. Li, A. Bandarenka, R. Fischer, Chem. Asian J. 14 (2019) 3474–3501.
[14] L. Zhang, J. Xiao, H. Wang, M. Shao, ACS Catal. 7 (2017) 7855–7865.
[15] Y. Liu, Y. Su, X. Quan, et al., ACS Catal. 8 (2018) 1186–1191.
[16] S. Mukherjee, D. Gullen, S. Karakalos, et al., Nano Energy 48 (2018) 217–226.
[17] P. Song, L. Kang, H. Wang, R. Guo, R. Wang, ACS Appl. Mater. Interfaces 11 (2019) 12408–12414.
[18] W. Guo, Z. Liang, J. Zhao, et al., Small Methods 2 (2018) 1800204.

[19] F. Yin, X. Lin, X. He, et al., Mater. Lett. 248 (2019) 109–113.
[20] R. Zhang, J. Han, B. Zheng, et al., Inorg. Chem. Front. 6 (2019) 391–395.
[21] Q. Qin, Y. Zhao, M. Schmallegger, et al., Angew. Chem. Int. Ed. 58 (2019) 13101–13106.
[22] Y. Gao, Z. Han, S. Hong, ACS Appl. Energy Mater. 8 (2019) 6071–6077.
[23] S. Luo, X. Li, B. Zhang, Z. Luo, M. Luo, ACS Appl. Mater. Interfaces 11 (2019) 26891–26897.
[24] S. Luo, X. Li, W. Gao, H. Zhang, M. Luo, Sustain. Energ. Fuels 4 (2020) 164–170.
[25] L. Jiao, H.L. Jiang, Chem 5 (2019) 786–804.
[26] Z. Geng, Y. Liu, X. Kong, et al., Adv. Mater. 30 (2018) 1803498.
[27] H. Tao, C. Choi, L.X. Ding, et al., Chem 5 (2019) 204–214.
[28] X. Zhao, F. Yin, N. Liu, et al., J. Mater. Sci. 52 (2017) 10175–10185.
[29] L. Zhao, X. Kuang, C. Chen, et al., Chem. Commun. 55 (2019) 10170–10173.
[30] Q. Cui, G. Qin, W. Wang, et al., J. Mater. Chem. A 7 (2019) 14510–14518.
[31] N. Lahiri, N. Lotfizadeh, R. Tsuchikawa, V.V. Deshpande, J. Louie, J. Am. Chem. Soc. 139 (2017) 19–22.
[32] X. Liu, J. Wang, J. Zhao, J.X. Zhao, Y. Liu, Appl. Surf. Sci. 487 (2019) 833–839.
[33] T. Kambe, R. Sakamoto, K. Hoshiko, et al., J. Am. Chem. Soc. 135 (2013) 2462–2465.
[34] A.J. Clough, J.W. Yoo, M.H. Mecklenburg, S.C. Marinescu, J. Am. Chem. Soc. 137 (2015) 118–121.
[35] H.K. Lee, C. Koh, Y.H. Lee, et al., Sci. Adv. 4 (2018) 3208.
[36] Y. Yang, S.Q. Wang, H. Wen, et al., Angew. Chem. Int. Ed. 58 (2019) 15362–15366.